Design of the VenSpec-H instrument on ESA's EnVision mission: development of critical elements, highlighting the FFCP and grating

Roderick De Cock*[a], Séverine Robert[a], Eddy Neefs[a], Justin Erwin[a], Michael Vervaeke[b], Hugo Thienpont[b], Etienne Renotte[c], Philippe Klinkenberg[c], Benoit Borguet[c], Solal Thomas[c], Wouter Moelans[d], Aaron Algoedt[d], Lieve De Vos[d], Ramatha Sørensen[d], Moshe Blau[d], Ann Carine Vandaele[a], Ian R. Thomas[a], Sophie Berkenbosch[a], Lars Jacobs[a], Pieter Bogaert[a], Bram Beeckman[a], Ansje Brassine[a], Neophytos Messios[a], Erwin De Donder[a], David Bolsée[a], Nuno Pereira[a], Bojan Ristic[a], Paul J. Tackley[e], Taras Gerya[e], Stefan Kögl[f], Paola Kögl[f], Hans-Peter Gröbelbauer[g], Florian Wirz[g], Gerhard Stefan Székely[h], Nick Eaton[i], Elena Roibás-Millán[j], Ignacio Torralbo[j], Higinio Rubio-Arnaldo[j], José Miguel Álvarez[j], Daniel Navajas Ortega[j], Daphne Stam[k], Jose M. Castro-Marin[l], Jaime Jiménez Ortega[l], Luisa Lara[l], Jörn Helbert[m], Giulia Alemanno[m], and Emmanuel Marcq[n]

[a]Royal Belgian Institute for Space Aeronomy, BIRA-IASB, Ringlaan 3, 1180 Brussels, Belgium
[b]Brussels Photonics, Department of Applied Physics and Photonics (B-PHOT – TONA) and Flanders Make, Vrije Universiteit Brussel, Pleinlaan 2, 1050, Brussels, Belgium
[c]AMOS, rue des Chasseurs Ardennais 2, 4031 Angleur, Belgium
[d]OIP Space Instruments, Westerring 21, 9700 Oudenaarde, Belgium
[e]Eidgenössische Technische Hochschule (ETH) Zürich, Rämistrasse 101, 8092 Zürich, Switzerland
[f]KOEGL Space, Gruebacherstrasse 13, 8157 Dielsdorf, Switzerland
[g]Fachhochschule Nordwestschweiz (FHNW), Klosterzeigstrasse 2, 5210 Windisch, Switzerland
[h]Hochschule Luzern (HSLU), Technikumstrasse 21, 6048 Horw, Switzerland
[i]Space Acoustics, Peterwise 3 8197 Rafz, Switzerland
[j]Instituto Universitario de Microgravedad "Ignacio Da Riva" (IDR/UPM), Universidad Politécnica de Madrid, 28040 Madrid, Spain
[k]Leiden Observatory, Niels Bohrweg 2, 2333 CA Leiden, The Netherlands
[l]Instituto de Astrofisica de Andalucia, IAA-CSIC, Glorieta de la Astronomia, 18008 Granada, Spain
[m]Deutsches Zentrum für Luft- und Raumfahrt e.V. Germany
[n]LATMOS/IPSL, UVSQ Université Paris-Saclay, Sorbonne Université, CNRS, Guyancourt, France

ABSTRACT

EnVision is ESA's upcoming mission to Venus with a launch scheduled in 2031. One of the payloads on board is the VenSpec suite,[1] containing three spectrometer channels, one of which is VenSpec-H. VenSpec-H (Venus Spectrometer with High resolution) performs absorption measurements in the atmosphere of Venus in four near-infrared spectral bands. VenSpec-H is developed under Belgian management and builds on heritage from instruments on Venus-Express and TGO. Techniques used in these precursor instruments are improved and complemented with new technologies to comply with the scientific goals of the EnVision mission. The operating

*Correspondence to roderick.decock@aeronomie.be

Infrared Remote Sensing and Instrumentation XXXII, edited by Marija Strojnik, Jörn Helbert, Proc. of SPIE Vol. 13144, 131440E · © 2024 SPIE
0277-786X · doi: 10.1117/12.3027637

wavelength range (1.15 - 2.5 μm) imposes stringent temperature requirements on the instrument to make nightside measurements below the Venus clouds possible. Most importantly, the spectrometer's optical components are held in a separate cold section inside the instrument, cooled down to $-45°C$, to remove thermal background from the signal. To avoid heat dissipation close to the spectrometer optics, the electronic boards are kept in a separate box. Besides that, some mechanisms, placed in the warmer part of the instrument at the entrance or exit of the cold section, had to be developed: a turn window unit to protect the interior of the instrument during the aerobraking phase of the mission, a filter wheel mechanism to select the spectral bands of interest, and an integrated detector-cooler-assembly to register the spectra. Some passive optical elements in the spectrometer had low technological readiness at the start of the project. One of them is a freeform corrector plate, used to compensate for aberrations introduced in the system by a parabolic mirror. This device is developed by the Brussels Photonics lab of VUB (Brussels) using a supply chain with shape adaptive corrective polishing and dedicated metrology. Another is the echelle grating, used to disperse the incoming light into its spectral components, which is built by AMOS. Both devices are highlighted in this article.

Keywords: Space instrumentation, EnVision, infrared spectrometer, free form corrector, grating

1. INTRODUCTION

The EnVision mission was adopted by ESA in the beginning of 2024 and with it the scientific instrument VenSpec-H (Venus Spectrometer with High resolution). Besides VenSpec-H, the Envision payload consists of two other spectrometers (VenSpec-M[2,3] and VenSpec-U[4,5]), together with VenSpec-H part of the VenSpec suite,[6,7] SRS (Subsurface Radar Sounder), VenSAR (Synthetic Aperture Radar) and a radio science experiment.

Venus-Express was ESA's previous mission to Venus and it contained the Belgian SOIR channel (part of the SPICAV instrument). SOIR was later succeeded by the NOMAD instrument, on board ESA's ExoMars Trace Gas Orbiter to Mars. Building on the success of SOIR and NOMAD, VenSpec-H introduces new technological developments some of them highlighted in this paper. We put emphasis on two challenging parts in the domain of optics and photonics, namely VenSpec-H's freeform corrector plate and grating.

2. WORKING PRINCIPLE

VenSpec-H is an infrared spectrometer, looking in the nadir direction. It will operate both at dayside and at nightside in the 1.15 - 2.5 μm wavelength range.

2.1 Scientific goals

The scientific goal of the instrument is to study the atmosphere of Venus both above and below the clouds in order to detect gases that relate to volcanism and surface interactions. This means that VenSpec-H will take measurements on the day and night side of the planet in four specific narrow bands, see Table 1.

Table 1: Wavelength range per band, SNR and altitude range both for day and nightside

	Goal spectral band		SNR binned	Altitude range
dayside	band#2a	2.34 - 2.42 μm	175	65-80 km
	band#2b	2.45 - 2.48 μm	175	
	band#4	1.37 - 1.39 μm	175	
nightside	band#1	1.165 - 1.18 μm	84	0-15 km
	band#2a	2.34 - 2.42 μm	220	30-45 km
	band#2b	2.45 - 2.48 μm	220	
	band#3	1.72 - 1.75 μm	122	20-30 km

A full description of the science objectives can be found in[8,9]

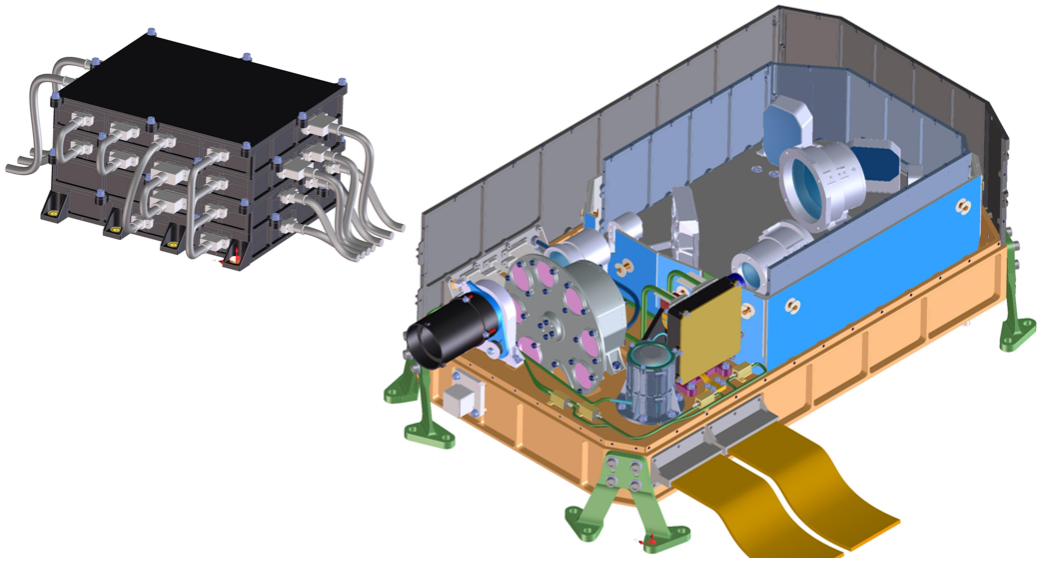

Figure 1: Instrument view of the electronic box and optical bench

2.2 Instrument concept

VenSpec-H consists of an optical bench with a warm section and a cold section and a separate stand alone electronic box, see Figure 1. The warm baseplate hosts the entrance optics and several mechanisms such as a turn window unit, a filter wheel mechanism, an integrated detector-cooler assembly with its associated proximity read-out electronics (DEP). In the cold section the spectrometer optics is located including a filter-slit-assembly, a free form corrector plate and a grating. The cold section is cooled down to $-45°C$, the warm section remains between $-10°C$ and $0°C$.
The electronic box contains a processor (PROC) and an FPGA (FPGA) board to control the instrument, a motor driver board (MOD) to operate the mechanisms and a power supply unit (PSU).

A more detailed description of VenSpec-H is available in.[1] The rationale behind the choice of the major optical components is explained in section 3.

2.3 Optical working principle

The optical design consists of three sections (see Figure 2):

1. band selector: a band of interest is selected by a filter in a filter wheel, situated in front of the spectrometer. Light passing through the filter is focused by the illumination optics onto the spectrometer entrance slit. A second part of the band selector, a set of two horizontal filter strips, is located at the same position as the spectrometer slit forming together the filter-slit assembly (FSA). A band selector in two stages is required because one of the used spectral bands is twice as large as the others, covering two instead of one spectral order. To avoid these orders from overlapping on the detector and to still be able to measure them simultaneously, this band is split horizontally in two.

2. spectrometer: converging light entering the spectrometer via the entrance slit (part of the FSA) falls on a parabolic mirror, where it is collimated. The parabolic mirror plays the role of collimator towards the spectral diffraction element, the echelle grating. Because the field-of-view of VenSpec-H is very elongated, the parabolic mirror introduces non-negligible aberrations at the extremes of the image. To correct these aberrations a freeform corrector plate is introduced in the optical path between the spectrometer slit and the parabolic mirror. At the exit of the grating sit the detector optics, consisting of two lens groups, that images and focuses the parallel light from the grating onto the detector. The spectrometer is cooled to suppress its thermal background.

3. detector: at the exit of the spectrometer sits an integrated detector-cooler assembly (IDCA). The detector registers the spectra that are produced in the instrument. The detector is cooled down actively to 135K to suppress as much as possible its dark current.

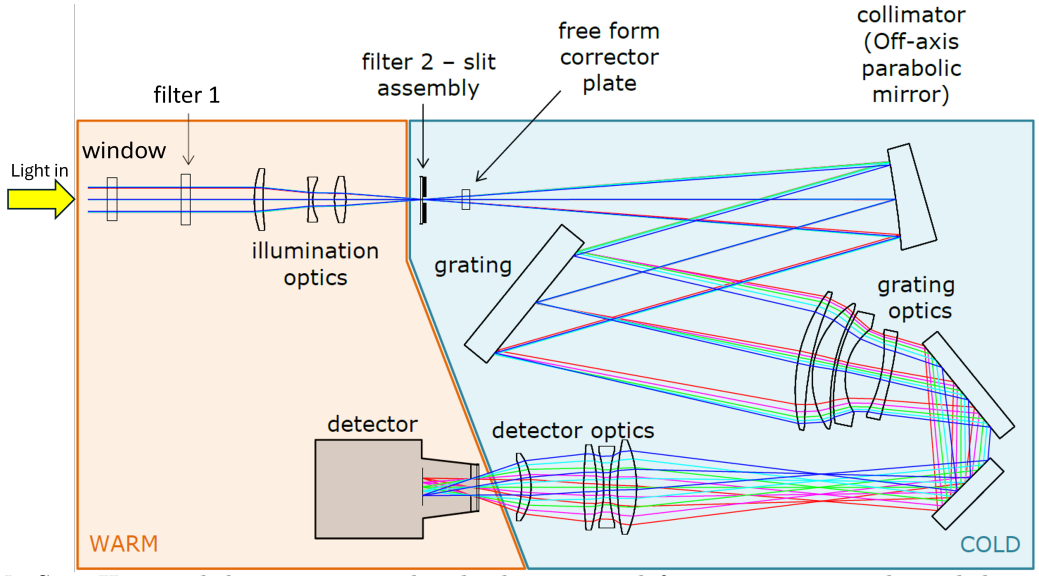

Figure 2: VenSpec-H optical design sections; band selection top left, spectrometer right and detector bottom left.

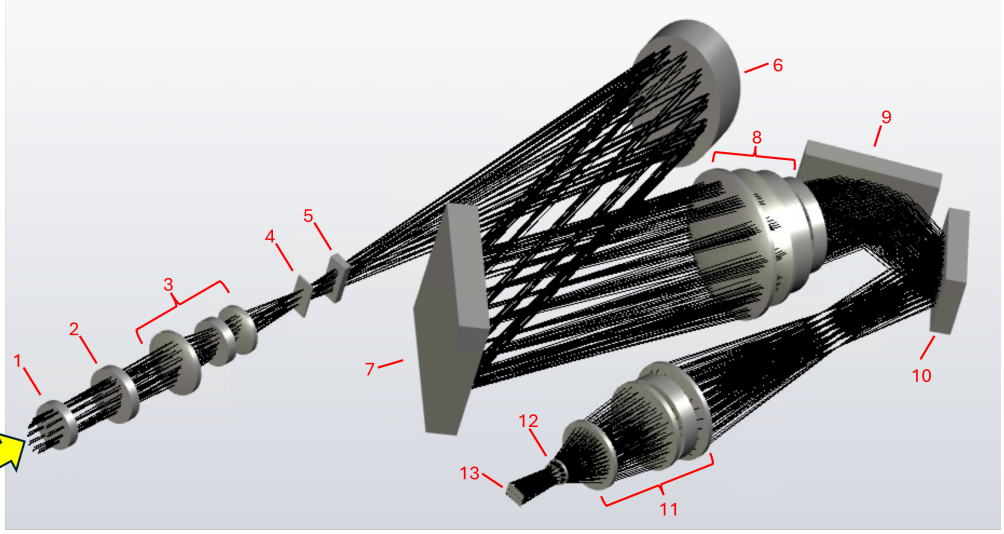

Figure 3: VenSpec-H optical working principle. Entrance optics: #1 is a window, #2 is one of the filters, #3 is the illumination optics. Spectrometer: #4 is a filter-slit assembly, #5 is a free form corrector plate, #6 is an off-axis parabolic mirror, #7 is an echelle grating, #8 is the grating optics, #9 and #10 are folding mirrors, #11 is the detector optics. Detector: #12 is a dewar entrance window and #13 is a focal plane array.

3. TECHNOLOGICAL DEVELOPMENTS

The instrument was designed around a number of new concepts in order to fulfil the stringent requirements on resolution and signal-to-noise ratio, needed mainly to be able to look through the clouds at the night side of Venus. This is done through so-called infrared night windows,[10] making the instrument operate in narrow

wavelength bands. An important driver is the fact that the spectrometer needs to be very cold ($-45°C$), a challenging temperature to have an FFCP, a grating and a filter-slit-assembly operate correctly.

Besides this, also a Filter Wheel Mechanism (FWM) had to be developed to do the band selection, rather then to use the heritage AOTF order sorter used in SOIR and NOMAD.
Unfortunately also a different Integrated Detector Cooler Assembly (IDCA) needed to be selected as the detector-cooler used in SOIR and NOMAD was discontinued.
Due to the extensive aerobraking phase at Venus, a Turn Window Unit (TWU) was developed to protect the instrument from atomic oxygen.

All six devices mentioned above are seen as critical subsystems of the instrument with low technological readiness level (TRL). ESA requires all critical subsystems to prove a TRL of 5 by the time of the Mission Adoption Review (MAR) which took place in the period October 2023 - January 2024, and a TRL of 6 by the time of instrument Preliminary Design Review (iPDR - planned in the period September - October 2025). For the VenSpec-H critical subsystems, the status at MAR is described below, in some more detail for the FFCP and the grating.

3.1 Cold section

Cooling down the instrument elements in front of the detector reduces the thermal background seen by the detector and the associated noise. All the optical elements (excluding the entrance optics) are therefore placed in a separate cold box, which is kept at $-45°C$. This temperature is achieved by passive cooling from a radiator on a cold face of the spacecraft Having big cold surfaces on a spacecraft in an orbit around Venus comes with certain challenges that have to be tackled by the spacecraft manufacturer.

This cold section is then carried by a bigger warm baseplate. The cold section and warm section are isolated thermally as much as possible, with the warm section staying between $-10°C$ to $0°C$. The warm section houses the entrance optics and the three abovementioned mechanisms: filter wheel mechanism, turn window unit and integrated detector-cooler assembly.

3.2 FFCP

The free form corrector (FFCP) plate is an optical element that corrects the distortions caused by the parabolic mirror further down the optical path. Moreover, it is needed to have a uniform distribution on the detector which allows for binning the data. This is done by adding up several/all rows together and consequently increasing the Signal to Noise (SNR) ratio. In SOIR and NOMAD no FFCP was needed because the field-of-view was quite proportional. In VenSpec-H the elongated field-of-view calls for an FFCP correction, hence, a design from scratch was needed and several early breadboards were developed by the VUB B-PHOT laboratory. The manufacturing process and requirements verification strategy are described below.

3.2.1 Material

The Freeform Corrector Plate was built in Heraeus Infrasil 302, a low OH-content fused silica for enhanced transmission in the IR bands of VenSpec-H.[11]

3.2.2 Integrated manufacturing/metrology process

The VUB B-PHOT laboratory features a freeform optics pilot-line, targeting innovations with advanced surface shaped optical components in polymers and glass materials. Key equipment for the FFCP are a 7-axis corrective polishing machine (CPM; IRP200 MKII from Zeeko LtD U.K., see Figure 4), a full-field interferometer (FFI; Verifire HDx from Zygo Ametek Corp. U.S., see Figure 9) and a white light interferometer with digital stitching (WLI; ContourGT-I 3D from Bruker Corp. U.S., see Figure 5) for surface shape error, surface microroughness and waviness characterisation , a coordinate measurement machine (CMM; Video Check UA from Werth Messtechnik GmbH DE, see Figure 6), a digital microscope (VIS; VHX-7000 digital microscope with VH-ZST zoom-lens system from Keyence Corp. JP, see Figure 8) for quality analysis on scratch/dig, bubbles and inclusions, chipping and other defects, and a polarimeter (POL; StrainMatic M4/90 from Illis GmbH DE) to characterize stress birefringes. Finally, a 5-axis milling and grinding station is used to remove the FFCP from the blank material and to shape its contours (MILL, RXP601DSHZ2 from Röders GmbH DE).

(a) Overview

(b) FFCP on the machine

(c) Close-up machine operating

Figure 4: CPM machine

The CPM is tied in a supply chain loop with the WLI as the surface generation process on the FFCP is inherently a corrective polishing process requiring feedback from metrology to design the next iteration in the polishing process. Given the surface radii, angles and size the shape adaptive grinding (SAG) technology[12–14] on the CMP was chosen to generate and polish the FFCP. This technology uses solid rubber tools cladded with diamond particles in a matrix. The latter can be a nickel or resin layer. Throughout the process both the particle size and matrix change from a hard and rough tool with $40\mu m$ grit in a nickel matrix, down to $3\mu m$ diamond grit on a resin layer. Towards the final microroughness figures SAG tools were chosen with different lapping cloths and CeriumOxide slurry as abrasive material.

The WLI uses partially coherent light to generate an interferogram with varying contrast allowing scanning a surface generating height map beyond the coherence length of the source. The WLI equipment has an automated turret with multiple objectives and a motorised stage allowing for digitally increasing the full field of view by stitching individual measurements. As such, the full FFCP can be measured during the process without using contact profilometry or computer generated holograms as an optical null element. The mathematical shape equation of the surface is subsequently subtracted from the raw data (see Figure 7) to generate the surface error map plot. Crucial to this step is coordinate system referencing. Therefore measurements are performed beyond the FFCP clear aperture (CA) until the flat, unmachined, area of the fused silica is in view. This flat unmachined area on the blank is specified with low roughness and sufficient flatness to serve as a reference plane to subtract tilt and set the Z-axis origin for the dataset. The XY axis origin is set by measuring fiducials on the blank.

The generated surface error map of the FFCP is subsequently used as an input in the computer aided design and manufacturing software of the CPM machine to generate a dwell time map for the tool in use. This dwell time map then modulates the toolpath speed over the FFCP surface depending on the removal rate of the SAG tool used.

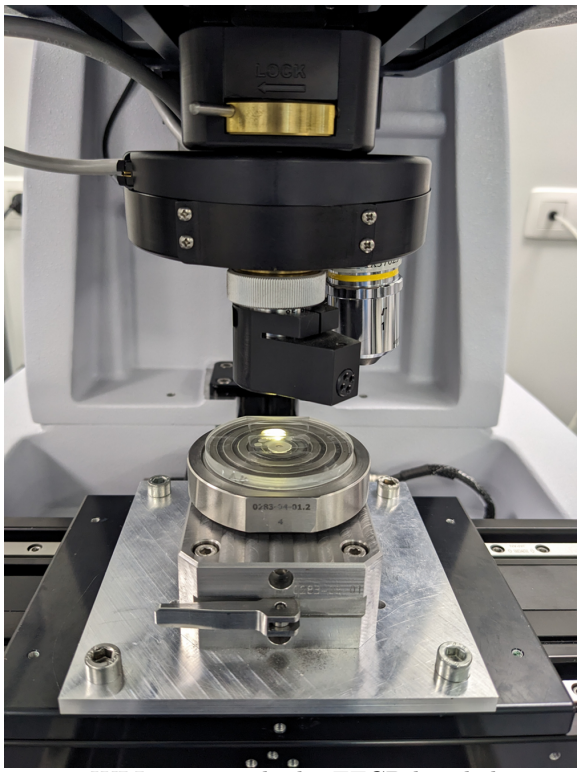

Figure 5: WLI setup with the FFCP bonded to a machining spigot

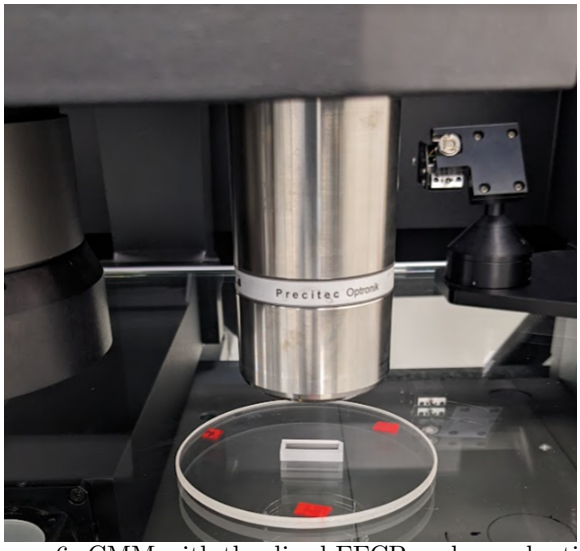

Figure 6: CMM with the diced FFCP under evaluation

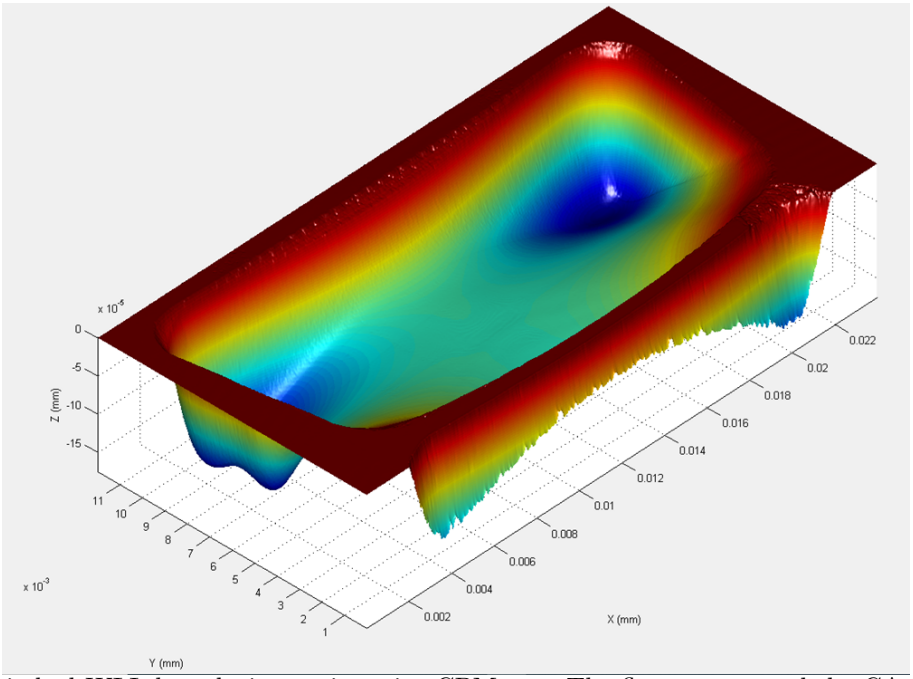

Figure 7: Raw stitched WLI data during an iterative CPM run. The flat area around the CA is measured as a Z-reference plane and the XY-coordinate system is fixed using fiducials on the blank.

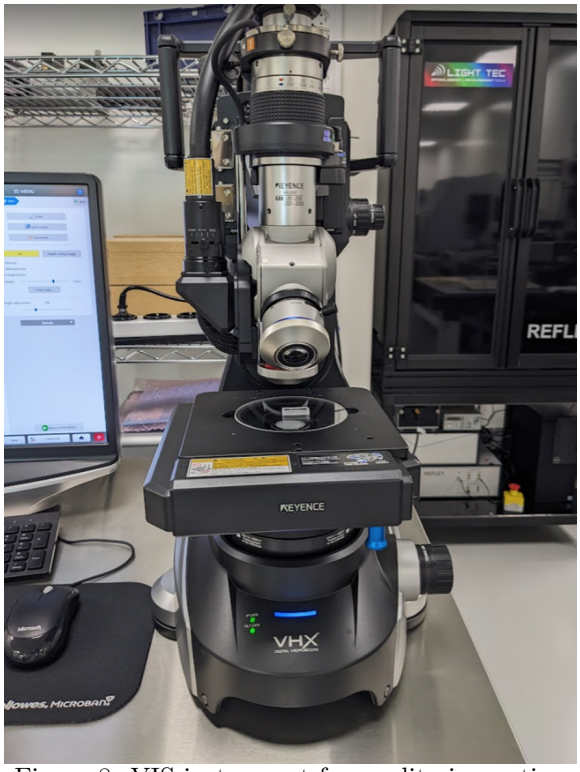

Figure 8: VIS instrument for quality inspection

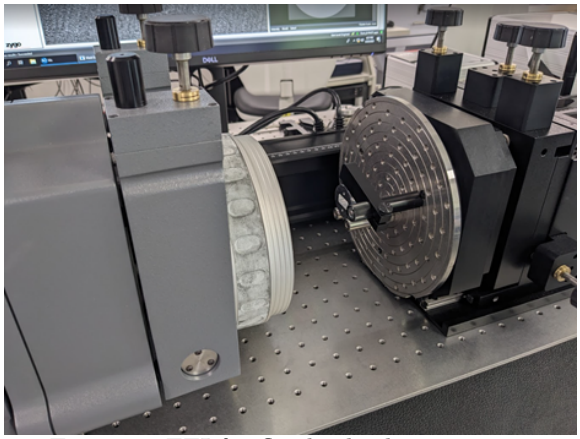
Figure 9: FFI for flat backside inspection

The careful observation of the surface error and surface roughness decrease led finally to a FFCP with a surface shape error according to ISO 10110: 3/5(-); $\lambda = 632,8nm$; RMSi $37nm$ (target RMSi $\leq 60nm$) , a surface roughness according to ISO 10110: 4.7 RMS from $1mm^{-1}$ to $1000mm^{-1}$ (target $\leq 5nm$) and a waviness figure according to ISO 10110: $8.6nm$ RMS from $0.18mm^{-1}$ to $5mm^{-1}$ in X (target $\leq 10nm$ RMS from $0.18mm^{-1}$ to $5mm^{-1}$). Subsequently the part was diced out in a grinding process on the MILL after which a full inspection including dimensional features and the flat backside was performed. One key parameter to control was the part thickness between the flat backside and the datum position on the freeform side as the corrective polishing process will gradually thin down the part. The initial specification was $4.00mm \pm 0.2mm$ with a goal to narrow the tolerance down to $4.00mm \pm 0.1mm$. With the knowledge gained during a number of test runs of the part the total volume to be removed could be estimated to match the surface quality specifications and at the same time keep the thickness under control. The final thickness measured using the CMM was $4.025mm$, well within the strongest specification.

3.3 Grating

The grating is the central part of the spectrometer where the incoming light is diffracted into its spectral components. The resulting spectral lines are projected on the columns of the detector. The advantage of using a high-dispersion echelle grating is that the full height of the detector can be used and so in-column binning can be done in case of weak signal to improve the SNR. Since the current design differs from the gratings used in SOIR and NOMAD (different line density, different blaze angle) and it has to be used at a completely different, low temperature, a breadboard model was developed by AMOS (see Figure 10). This demonstrator model was a reduced scale version ($50 \times 50mm$) without a holder (for the flight design the grating and holder will be one monolithic part). The manufacturing steps, are described below, focusing on the challenges faced during diamond machining and the specific problems encountered during the metrology of the optical surface.

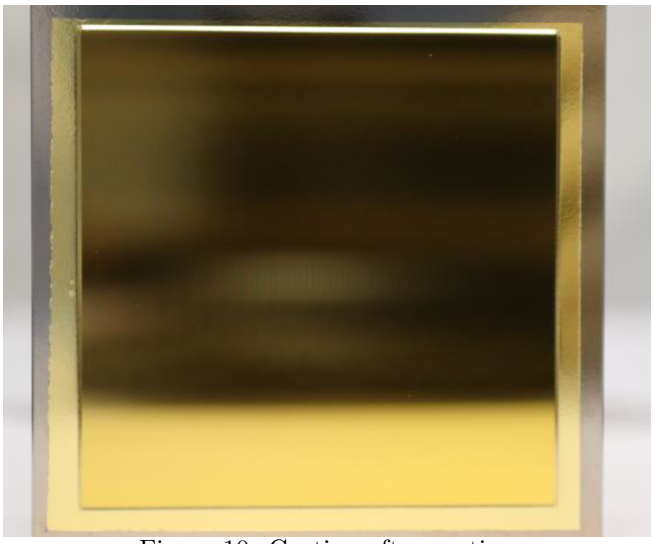

Figure 10: Grating after coating

Figure 11: Sauer DMU70-5 milling machine

Figure 12: Nanotech 350FG precision lathe

3.3.1 Material

The proposed solution for this application was an AlSi alloy substrate coated with nickel phosphor (NiP) plating. This solution allows for matching the thermal expansion coefficients of both materials, significantly mitigating figure variations related to the so-called bimetallic effect. Finally, the optical surface is coated with an unprotected gold layer.

3.3.2 Manufacturing process

Manufacturing started with milling substrate parts on a Sauer DUM70-5 5-axis machine (see Figure 11) followed by a first diamond machining operation on a Nanotech 350FG precision lathe (see Figure 12), aimed at achieving the accurate dimensions required for the next steps. After NiP plating, a new round of diamond turning was carried out, enabling the finishing of the precision reference surfaces (used for alignment) and mounting interfaces. Regarding the optical surface, it was first cut flat before considering the last "ruling" (or "grooving") operation.

The "ruling" operation was performed with a custom diamond tool cutting off the material of the NiP plating. The cutting tool has been specifically chosen to ensure the required groove profile (blaze angle and counter blaze)

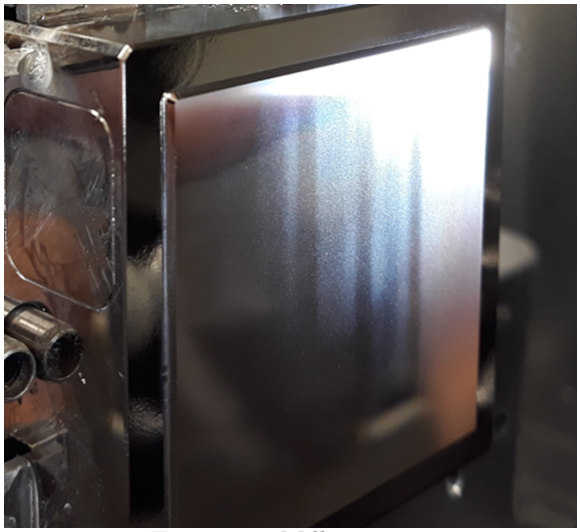

Figure 13: Milky aspect

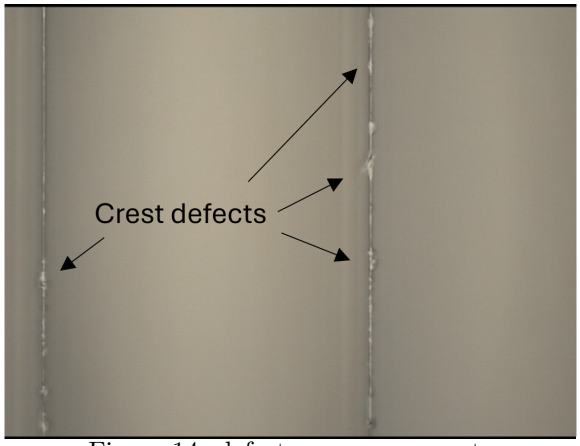

Figure 14: defects on groove crests

is achieved in a single pass. Special attention was devoted to ensuring the sharpness of the crests. During the first cuts, a milky aspect was observed on parts of the grooved surface. This effect was not apparent from the tool entry edge but the aspect progressively downgraded as the tool ran along the grooves (see Figure 13). Closer inspection revealed that this milky effect is related to the quality of the crests (see Figure 14). Fine tuning of the cutting parameters has been conducted on spare parts optimising diamond machining (DM) cutting conditions, modifying both depth of cut (DOC) and feed rate to achieve sharp edges and reduce their possible influence on stray light.

In principle, during the grooving step, several successive cuts can be performed on the same part, considering the small amount of material removed and the relatively high NiP plating thickness (typically $80\mu m$). This decreases the risk of discarding parts in case of poor grooving performance. In this specific case, the grooves were particularly deep ($20\mu m$) which left few chances for mistakes and repetitive trials. To manage the risk, it was decided to ask for spares with $80\mu m$- and $150\mu m$-thick NiP plating. This allowed as well to compare manufacturing performance between both conditions.

Compared to former AMOS experience, achieving low roughness levels along the grooves proved to be more difficult for such echelle gratings (best roughness around $5-6nm$ RMS where $< 3nm$ RMS can routinely be achieved for echelette grating designs). Several parameters, among which depth of cut, feed rate, steep angles, and cutting configuration are likely to influence cutting performance. A clear correlation with a specific parameter could however not be pointed out within the timeframe of the project.

3.3.3 Metrology methods

The surface morphology, i.e., the shape of the grooves and the groove patterns was measured with a Keyence VK-X3000 confocal microscope (see Figure 15) and a Nomad white light interferometer from Zygo (see Figure 16).

Regarding measurements with the confocal microscope, the specific geometry of the optical surface, with blaze angle close to 45-50 degrees, implies parasitic reflections that must be managed properly. Moreover, the depth of the grooves ($20\mu m$) proved to be quite challenging being very close to the Keyence vertical range. Further proper lateral calibration had to be considered to characterise the grating period accurately.

One of the most important requirement for the demonstrator grating was a low cumulative error on the grating period. Considering the tight specification, this characterisation proved to be particularly challenging to assess, as it required to measure with an accuracy well below 1 micron over a macroscopic surface.

This measurement was performed by using the microscope embedded on the diamond turning machine and by indexing positions from the initial groove. By far, the positioning accuracy of a precision lathe is the best

Figure 15: Keyence VK-X3000 laser scanning 3D confocal microscope for groove profile measurements

Figure 16: Nomad WLI by Zygo for roughness along the grooves

available (around $\pm 10nm$). Precision of the measurement was limited by the resolution of the images from the microscope.

3.3.4 Importance of cleanliness

Cleanliness is of primary importance when manufacturing gratings. Apart from purely cosmetic concerns, a clean surface is critical before coating. Special care must be devoted ensuring suitable environmental conditions. Gratings are particularly sensitive to contamination because of their specific surface morphology and surface tension effects related to the μm-scale. Contaminants can easily be trapped into the grooves and classical cleaning methods, in addition to the involved extra damage risks, can suffer limited efficiency.

Fluids used when diamond machining can dry on the surface and in the grooves, which makes the optical surface very difficult or even impossible to clean. Specific procedures were designed to get rid of deleterious effects related to drying.

A clear demonstration of the importance of proper and detailed inspection after machining was given after gold coating, as one of the two coated parts revealed a limited delamination from the edges (see Figure 17). During post-inspection, presence of contaminants in the grooves was evidenced in the area where delamination occurred (see Figure 18).

3.4 Filter-Slit Assembly (FSA)

A third critical optical component is the filter-slit assembly (FSA). The assembly consists of a slit, slightly curved to compensate for the smile of the optical system and assures that the spectral lines appear straight on the detector, nicely aligned with the columns. The slit is deposited on top of a double horizontal pair of filter bands, that split spectral band #2, the one that spans two grating orders, into band #2a and band #2b, allowing for the full band to be measured in one go. In between sits a black strip to prevent cross-talk between

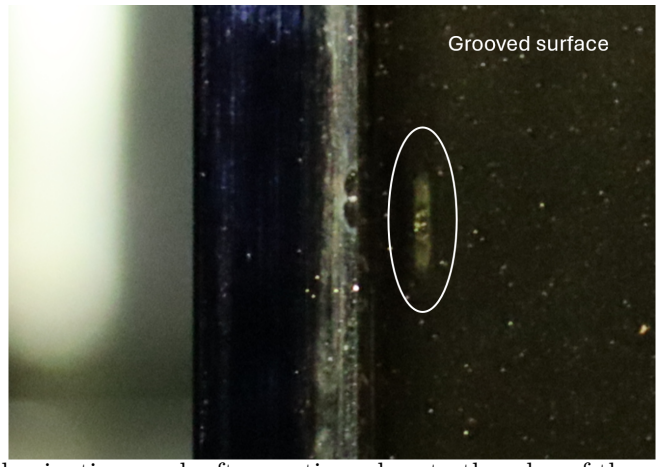

Figure 17: Delamination mark after coating, close to the edge of the grooved surface

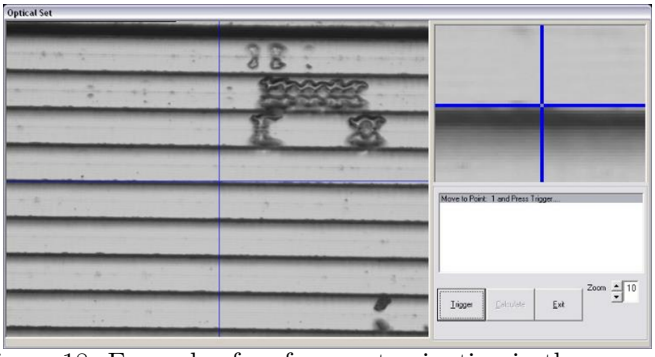

Figure 18: Example of surface contamination in the grooves

the two bands. This assembly will be manufactured using existing techniques. Therefore, a breadboard will be developed only in a later phase, together with all the other "standard" optical elements in the optical path.

3.5 Filter Wheel Mechanism (FWM)

In SOIR and NOMAD an acousto-optical tunable filter (AOTF) was used to select individual grating orders, i.e., the spectral bands of interest. However, a feasibility study showed that, given the very specific science and mission constraints, an AOTF was not a viable option for VenSpec-H. Knowing that VenSpec-H just has to look at four spectral bands and not a continuous wavelength range, a filter wheel mechanism was chosen instead. The FWM must hold the different filters that will be used and will also have an open and a closed position for calibration purposes. The FWM will be used intensively during flight, having to move from one filter to another as fast as possible and with a position repeatability of less than $0.1mm$. This leads to a high required number of revolutions. The development of a breadboard FWM was done under the responsibility of the Lucerne University of Applied Sciences and Arts (HSLU, Switzerland) and is described in detail in.[15,16]

3.6 Integrated Dewar Detector Cooler (IDCA)

Due to the discontinuation of the detector-cooler used on SOIR and NOMAD, a different detector had to be selected. The selected IDCA is an MCT (Mercury Cadmium Telluride) detector with a linear cryocooler. It is a slightly modified COTS (Commercial Of The Shelf) product from AIM (Germany). Four engineering models were built, one of them carrying only the read-out integrated circuit, the three others the full detector, consisting of focal plane array and ROIC. All four devices are mounted in a vacuum tight dewar, with a transparent window at the entrance. The detectors sit at the tip of a cold finger that extracts heat from the detector. Heat is pumped out from the rear of the cold finger, over a transfer tube, by a self-standing dual piston linear compressor.

The cooler's lifetime is in line with the expected mission duration and number of operational cycles. The focal plane array will be cooled down typically to a temperature between 120 and $135K$. One of the delivered engineering models will undergo standard qualification tests against the mission environment.

A full characterisation of the detector will be done by the Netherlands Institute for Space Research (SRON, Netherlands). Dedicated space qualified electronics will be developed in Belgium and Czech Republic to drive the cooler and read-out the detector.

3.7 Turn Window Unit (TWU)

The EnVision spacecraft will be slowed down and brought into its final science orbit by means of a long aerobraking sequence. During the consecutive dips in the atmosphere there is a risk of atomic oxygen contamination through the open aperture of the instrument. Therefore, a TWU was developed that holds a window right behind the aperture, protecting the interior against the atomic oxygen fluence. After the aerobraking phase, the mechanism will be activated and the window slung out of the optical path. The mechanism is one-shot and it is based on the thermal knife principle. A polymer wire under spring tension keeps the window in place. Upon activation, this wire is melted by applying electrical power to a thermal element. The spring force will rotate the mechanism until it is out of the optical path and hits a hard stop. The spring force will keep it in that final end position. The option could have been taken to have a full metal door, but having a window in the mechanism provides an additional fail safe solution in the contingency case that the door would not open. Also with the door closed, the continuation of the mission is not jeopardised and the science not degraded. The development of this mechanism is done by the Deutsches Zentrum für Luft- und Raumfahrt (DLR, Germany).

4. FUTURE ACTIVITIES IN THE DEVELOPMENTS

As stated earlier, the status at MAR is presented here and further developments are needed to reach a TRL of 6 by iPDR. All the mechanisms (FWM, IDCA, TWU) are progressing to TRL 6, the completion of the currently ongoing development activities is sufficient. For the optical critical components (FFCP, grating, FSA), a dedicated test with the full optical path needs to be done. This is because the performance of the individual components is impossible to measure stand-alone. Instead it is opted do develop a breadboard of the full optical path and to performance test it in real operational conditions, i.e., in vacuum and at $-45°$. The existing FFCP breadboard will be re-used, for the grating a full scale model will need to be manufactured including a monolithic holder and for the FSA, and all the other optical parts, first-time parts will be ordered and/or manufactured.

In the later project phases, flight models will be made of all the abovementioned elements with slight optimisations and tweaking where needed.

5. CONCLUSIONS

The design of VenSpec-H is concisely presented, followed by a description of the technological developments of critical subsystems that were performed. The free form corrector plate (FFCP) and grating are discussed in more details, highlighting the challenges in the production process and the metrology method. For both parts breadboard models were successfully manufactured, meeting the technical specifications. The other critical subsystems are described in lesser detail. Confidence exists today that all elements are well on track to prove technological maturity in the short future. the three passive optical critical subsystems, FFCP, grating and filter-slit assembly will be integrated in the coming months in an overall breadboard of the optical path. It can be concluded that the different manufacturers and suppliers have proven manufacturability of the devices, and their individual functional criticalities and operability concerns have been reduced.

6. ACKNOWLEDGEMENTS

The VenSpec-H development is under the responsibility of a Belgian Instrument Lead team (BIRA-IASB, Brussels). Contributions are provided by research institutes or industrial companies in Europe:

- in Switzerland: ETHZ, KOEGL Space, FHNW, HSLU, and Space Acoustics;

- in Spain: IDR-UPM and IAA-CSIC;
- in The Netherlands: Leiden Observatory;
- in Germany: DLR and AIM;
- in Belgium: OIP, AMOS and B-PHOT VUB.

Support was also received from the EnVision (study and) project team and the PRODEX team at ESTEC.

The optical design work and the development of the FFCP, the grating and the TWU are made possible thanks to funding by the Belgian Science Policy Office (BELSPO). The development of the FWM is made possible thanks to funding by the Swiss Space office (SSO). The European Space Agency (ESA) was in charge for the purchase of the IDCA.
VenSpec-H work not specifically mentioned in this paper (e;g., mechanical and electrical development), falls under funding from the Belgian Science Policy Office (BELSPO) (Prodex Experiment Agreement C4000128137), the Swiss Space office (SSO) (Prodex Experiment Agreements 4000138690, 4000138246 and 4000138247) and the Spanish Agencia Estatal de Investigación (grants PID2021-126365NB-C21 and PID2021-126365NA-C22). Funding from Belgium and Spain was financially and contractually coordinated by the ESA Prodex Office.

EM acknowledges support from CNES and ESA for all EnVision-related activities.

REFERENCES

[1] Neefs, E., Vandaele, A. C., De Cock, R., Erwin, J., Robert, S., Thomas, I. R., Berkenbosch, S., Jacobs, L., Bogaert, P., Beeckman, B., Brassine, A., Messios, N., De Donder, E., Bolsée, D., Pereira, N., Tackley, P. J., Gerya, T., Kögl, S., Kögl, P., Gröbelbauer, H.-P., Wirz, F., Székely, G., Eaton, N., Roibás-Millán, E., Torralbo, I., Rubio-Arnaldo, H., Alvarez, J. M., Navajas Ortega, D., De Vos, L., Sørensen, R., Moelans, W., Algoedt, A., Blau, M., Stam, D., Renotte, E., Klinkenberg, P., Borguet, B., Thomas, S., Vervaeke, M., Thienpont, H., Castro-Marin, J. M., and Jimenez, J., "VenSpec-H spectrometer on the ESA EnVision mission: Design, modeling and analysis," *Acta Astronautica (accepted)* (2024).

[2] Hagelschuer, T. et al., "The Venus Emissivity Mapper (VEM): Instrument design and development for VERITAS and EnVision," in [*Infrared Remote Sensing and Instrumentation XXXII*], **This volume**, International Society for Optics and Photonics, SPIE (2024).

[3] Helbert, J., Säuberlich, T., Dyar, M. D., Ryan, C., Walter, I., Reess, J.-M., Rosas-Ortiz, Y., Peter, G., Maturilli, A., and Arnold, G., "The Venus Emissivity Mapper (VEM): advanced development status and performance evaluation," in [*Infrared Remote Sensing and Instrumentation XXVIII*], Strojnik, M., ed., *Society of Photo-Optical Instrumentation Engineers (SPIE) Conference Series* **11502**, 1150208 (Aug. 2020).

[4] Lustrement, B. et al., "Design of the VenSpec-U instrument: A double UV imaging spectrometer to analyze sulfured gases in the Venus' atmosphere," in [*Infrared Remote Sensing and Instrumentation XXXII*], **This volume**, International Society for Optics and Photonics, SPIE (2024).

[5] Marcq, E., Montmessin, F., Lasue, J., Bézard, B., Jessup, K. L., Lee, Y. J., Wilson, C. F., Lustrement, B., Rouanet, N., and Guignan, G., "Instrumental requirements for the study of Venus' cloud top using the UV imaging spectrometer VeSUV," *Advances in Space Research* **68**(1), 275–291 (2021).

[6] Helbert, J. et al., "The VenSpec Suite Organization: Collaborative development from instrument proposal to scientific analysis," in [*Infrared Remote Sensing and Instrumentation XXXII*], **This volume**, International Society for Optics and Photonics, SPIE (2024).

[7] Fitzner, A. et al., "Electrical integration of the VenSpec Spectrometer consortium: an architecture trade-off," in [*Infrared Remote Sensing and Instrumentation XXXII*], **This volume**, International Society for Optics and Photonics, SPIE (2024).

[8] Helbert, J., Vandaele, A. C., Marcq, E., Robert, S., Ryan, C., Guignan, G., Rosas-Ortiz, Y., Neefs, E., Thomas, I. R., Arnold, G., Peter, G., Widemann, T., and Lara, L., "The VenSpec suite on the ESA EnVision mission to Venus," in [*Infrared Remote Sensing and Instrumentation XXVII*], Strojnik, M. and Arnold, G. E., eds., **11128**, 1112804, International Society for Optics and Photonics, SPIE (2019).

[9] Robert, S. et al., "Scientific objectives and instrumental requirements of the IR spectrometer VenSpec-H onboard EnVision," in [*Infrared Remote Sensing and Instrumentation XXXII*], **This volume**, International Society for Optics and Photonics, SPIE (2024).

[10] Bézard, B. and de Bergh, C., "Composition of the atmosphere of venus below the clouds," *Journal of Geophysical Research: Planets* **112**(E4) (2007).

[11] Schlichting, W., Kühn, B., and Nürnberg, F., "Optimized fused silica used in new astronomical applications," in [*Advances in Optical and Mechanical Technologies for Telescopes and Instrumentation V*], Navarro, R. and Geyl, R., eds., **12188**, 1218803, International Society for Optics and Photonics, SPIE (2022).

[12] Beaucamp, A., Namba, Y., Combrinck, H., Charlton, P., and Freeman, R., "Shape adaptive grinding of cvd silicon carbide," *CIRP Annals - Manufacturing Technology* **63**, 317–320 (12 2014).

[13] Beaucamp, A., Namba, Y., Charlton, P., Jain, S., and Graziano, A., "Shape adaptive grinding (sag) of complex additively manufactured parts," *Proceedings - ASPE 2015 Spring Topical Meeting: Achieving Precision Tolerances in Additive Manufacturing* , 141–146 (01 2015).

[14] Zhu, W. and Beaucamp, A., "Compliant grinding and polishing: A review," *International Journal of Machine Tools and Manufacture* **158**, 103634 (11 2020).

[15] Székely, G. S., Eberli, R., Grossmann, M., Tenisch, S., Hans-Peter Gröbelbauer, F. W., Seiler, P., Kögl, P., Kögl, S., Tackley, P. J., Gerya, T., Vandael, A.-C., and Neefs, E., "VenSpec-H Filter Wheel Mechanism Breadboard Development and Test," *Proceedings of the 47th Aerospace Mechanisms Symposium* , 459–472 (15-17 May 2024).

[16] Székely, G. S., Neefs, E., Eberli, R., Grossmann, M., Tenisch, S., Gröbelbauer, H.-P., Wirz, F., Seiler, P., Kögl, P., Kögl, S., Jacobs, L., Berkenbosch, S., Vandaele, A.-C., Tackley, P., Gerya, T., Cock, R. D., Erwin, J. T., Robert, S., and Pereira, N., "Development of a Filter Wheel for VenSpec-H," in [*Infrared Remote Sensing and Instrumentation XXXII*], International Society for Optics and Photonics, SPIE (2024).